Control of Porous Morphology in Suspension Polymerized Poly(divinylbenzene) Resins Using Oligomeric Porogens

Fiona S. Macintyre and David C. Sherrington*

Department of Pure and Applied Chemistry, University of Strathclyde, Glasgow G1 1XL, Scotland, UK

Received May 7, 2004; Revised Manuscript Received June 28, 2004

ABSTRACT: Porous poly(divinylbenzene) (DVB) resins have been prepared using suspension polymerization with toluene and an oligomer as coporogens. The oligomers investigated were poly(propylene glycol) 1000 (PPG 1000), poly(propylene glycol) 4000 (PPG 4000), and poly(dimethylsiloxane) (PDMS). The porogen was used in a 1/1 vol/vol ratio with DVB, and with each oligomeric coporogen the full compositional range 100 vol % toluene to 100 vol % oligomer was examined. As predicted from previous knowledge of the effect of different solvent porogens, toluene yielded a highly microporous resin with a large dry state surface area (∼650 m^2 g^{-1}), whereas each oligomeric porogen yielded a highly macroporous resin with rather low surface area ∼15−50 m^2 g^{-1}. Using mixtures of toluene and oligomer as coporogens, we speculated that it might be possible to produce a resin with a strongly bimodal pore size distribution with one population of pores in the micropore region, and one in the macropore region. This proved to be the case with a mixture 80 vol % toluene and 20 vol % PDMS. Unexpectedly, however, the surface area of the poly(DVB) resins was found to rise significantly (∼100 m^2 g^{-1}) in shifting from toluene as sole porogen to a mixture with a low level of oligomeric coporogen (∼4−6 vol %). Further increase in the level of oligomer led to the predicted fall in surface area. Overall, therefore, it is clear that use of oligomers, particularly as coporogens with solvent porogens, provides a valuable methodology for fine-tuning the porous morphology of poly(DVB) resins.

Introduction

"Macroporous" polystyrene-based ion-exchange resins were first introduced almost simultaneously from three industrial laboratories around 1960.[1−3] Since then, they have become widely used in applications ranging from large-scale water treatment through to pharmaceutical products.[4] Most recently, they have proved their value as supports for catalysts, reagents, and scavenging species in organic chemistry where they have considerably facilitated the overall synthetic process[5,6] and allowed the implementation of robotic handling and other high throughput methodologies.[7] The term "macroporous resin" is now an unfortunate one but was coined to indicate that these resins possess a permanent pore structure even in the dry state, distinguishing them from earlier "gel-type resins" which are swollen gels that collapse to an essentially nonporous state when dry. In this paper we shall restrict our use of the terms micro-, meso-, and macropore to that defined by IUPAC (i.e., micropores < 2 nm; 2 nm < mesopores > 50 nm; macroporous > 50 nm diameter), and we shall refer to "macroporous" resins as porous resins. The process by which the latter are formed is complex and involves simultaneous vinyl polymerization, cross-linking, phase separation, microgel fusion (and aggregation), and pore in-filling. As a result, in general, the final product has a broad pore size distribution often ranging from micropores right through to macropores. The use of an organic solvent as a porogen or pore-former, and the resulting phase separation induced during polymerization, is a crucial factor in controlling the average pore diameter and corresponding internal surface area of a resin. As a general guide, solvent porogens with poor thermodynamic compatibility with the incipient polymer network cause early phase separation and microgel formation. This allows the microgel particles to fuse, aggregate, and become in-filled during the ensuing polymerization (i.e., the morphological structure coarsens). Overall, therefore, this gives rise to the formation of pores with large average diameter and resins with rather low surface area (say <50 m^2 g^{-1}; N_2 sorption, BET). In contrast, solvent porogens with good thermodynamic compatibility with the polymer network cause phase separation at a much later stage in the polymerization, and so the microgel particles, though still becoming fused, tend to retain more of their individuality (i.e., the morphological structure does not coarsen). As a result, the average pore diameter is much lower and the surface area of such resins larger (up to ∼750 m^2 g^{-1}). Further details on morphology control in resins prepared by suspension polymerizations are available in the literature.[8−10]

Interestingly, very few pairs of (different) homopolymers are thermodynamically compatible; indeed, the rule of thumb is that different hompolymers are *highly* incompatible. This raises the possibility of using linear homopolymers as polymeric porogens in resin synthesis where, by analogy with solvent porogens, early phase separation might be expected and in due course the formation of large pores and low surface area porous resins. Indeed, a number of groups have reported the use of polymers as porogens. A review of the early work on such porogens[11] did indeed report that ∼20 vol % of polystyrene, poly(methyl methacrylate), or poly(vinyl acetate) in a styrene (St)/divinylbenzene (DVB) (10%) suspension polymerization, following removal of the porogen, yields a resin with a porosity of ∼30%, and surface area typically < 5 m^2 g^{-1}, indicative of large pores. Interestingly, the molar mass of the polystyrene porogen had to be >50K to generate this morphology, whereas an oligomer of molar mass ∼ 5K was reported to behave more like a solvent porogen. A major problem in using polymeric porogens is that the viscosity of the

* Corresponding author: e-mail d.sherrington@strath.ac.uk.

10.1021/ma0491053 CCC: $27.50
Published on Web 09/03/2004

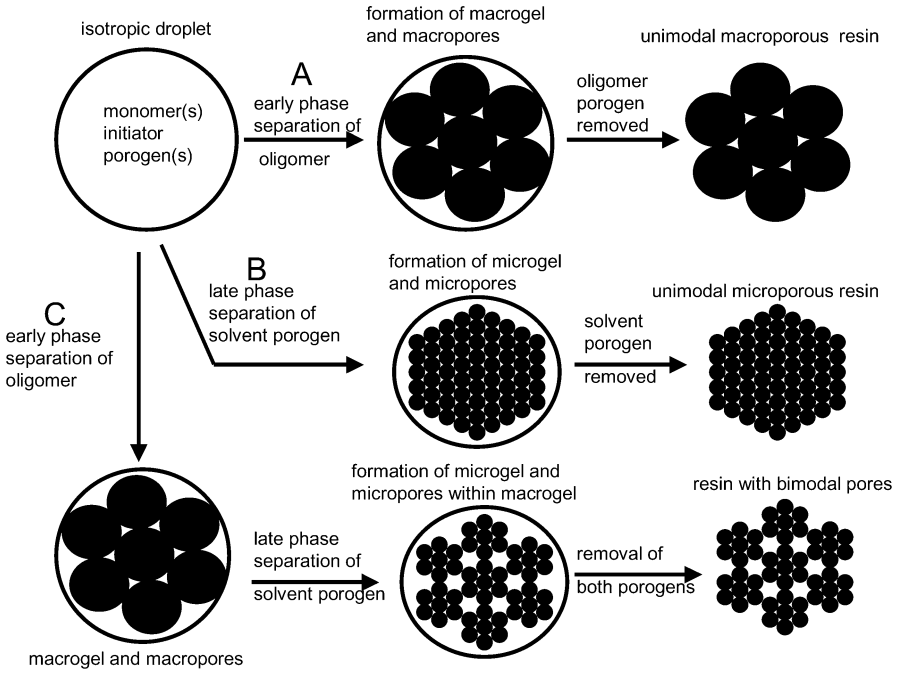

Figure 1. Schematic representation of pore formation in poly(DVB) resins: A, using an oligomeric porogen; B, using a thermodynamically "good" solvent porogen; C, using a solvent and an oligomer as coporogens.

comonomer mixtures rises sharply as the weight percent of these porogens is increased such that efficient dispersion into, and retention of, spherical droplets becomes a major problem. In addition, a limited weight percent of porogen thence yields a low pore volume in the resulting resin. As a result, it has become more usual to use polymeric porogens in combination with solvent porogens.

Sederel and Jong[12] used polystyrenes with molar mass 33−140K in toluene, and also in hexane, as coporogens and showed an increase in the pore size of the resins produced with St/DVB (10−25%). Likewise, Poinescu et al.[13] found a similar effect when using poly(vinyl acetate)s in C_{10}−C_{11} aliphatic alcohols as coporogens again in synthesizing St/DVB (10−15 vol %) resins. The elegant work by Svec et al.[14] using polystyrenes and a poly(methyl methacrylate) as porogens, primarily with toluene as solvent coporogen, in glycidyl methacrylate/ethylene glycol dimethacrylate resin syntheses demonstrated the problems of high viscosity in the dispersed organic phase. In this instance, even with relatively low levels of polymeric porogen, it was difficult to obtain a high-quality spherical resin product. More recently, however, Ferreira and co-workers[15] have succeeded in producing a spherical beaded product with these comonomers, in this instance employing polystyrene as the porogen in toluene as coporogen. The presence of the polymeric porogen again increased the average pore size, but decreased the pore volume, whereas surface areas were less affected. Perhaps the most significant use of polymeric porogens in controlling resin bead porous morphology has been in the methodology for producing beads with a unimodal size distribution. In these "seeded"[16] or "staged templated"[17,18] suspension polymerizations, inspired by the original methodology of Ugelstad et al.,[19] a monodisperse emulsion or dispersion polymer (usually a linear polystyrene) is used as vehicle to carry out e.g. a St/DVB polymerization with the "seed" or "template" acting to generate a monodisperse spherical poly(St−DVB) mimic with controlled porous morphology. In most cases an important constituent is dibutyl phthalate, which has poor thermodynamic compatibility with incipient poly(St−DVB) network, and it is not entirely clear that the linear polystyrene "seed" or "template" particle fully dissolves in the St/DVB comonomer mixture. Nevertheless, the meticulous work by the Berkeley group[17] seems to confirm this. Indeed, the polystyrene component, as well as acting as a former for the poly(St−DVB) network, certainly contributes to the evolution of the morphology of the latter.

We felt that oligomeric, rather than polymeric, porogens presented on an opportunity to avoid some of the problems associated with high molar mass porogens and might, for example, be used alone over a wide composition range without causing viscosity problems in the suspension polymerization and without limiting the pore volume of the product. We also felt that choice of an appropriate oligomer with toluene as a solvent coporogen might allow a double phase separation to occur during polymerization of DVB. The oligomeric porogen might induce an early phase separation, yielding in due course "macrogel" particles and macropores, while the toluene would phase separate much later (in the normal manner), yielding microgel and micropores. If this were to occur, a clearly bimodal distribution of pores would result (Figure 1C). Use of the oligomeric porogen along might be expected to produce a relatively narrow pore size distribution in the macropore region (Figure 1A). As we shall see, these effects can be realized, and as a bonus, low levels of oligomeric coporogen with toluene as primary porogen improves the connectivity of the fine pore structure that is formed, with a concomitant rise in the surface area.

Poly(ethylene glycol)s (PEGs) were obvious candidates as oligomeric coporogens, and indeed use of these has been reported[20] in the synthesis of porous poly(dimethylacrylamide)s in capillaries for electrochromatography. However, these polymerizations were in water/formamide solution. PEGs are also now being reported as useful porogens in the synthesis of porous monoliths[21] where again the Berkeley group are making a strong

Table 1. Poly(DVB) Resin Syntheses and Solid-State Porosity and Solvent Uptake Data

resin code	oligomer in porogen (vol %)[a]	yield of beads (%)	surface area: N_2 BET ($m^2\ g^{-1}$)	surface area: Hg intrusion ($m^2\ g^{-1}$)	surface area: total ($m^2\ g^{-1}$)	surface area: large pores (%)	av pore size (nm): N_2 BJH	av pore size (nm): Hg intrusion	porosity (%): N_2 BJH[b]	porosity (%): Hg intrusion	solvent uptake (g/g): toluene	solvent uptake (g/g): *n*-hexane
R1-TOL	0	75.0	660	141	801	17.6	3.6	12.0	28	32	0.45	0.34
R2-4PPG-1K	PPG1000,4	91.1	730	175	905	19.4	4.6	14.6	41	41	0.89	0.68
R3-5PPG-1K	PPG1000,5	86.9	700	156	856	18.2	4.6	15.4	38	40	0.79	0.58
R4-6PPG-1K	PPG1000,6	86.9	815	169	984	17.1	4.8	15.4	44	43	0.86	0.65
R5-7PPG-1K	PPG1000,7	94.6	760	194	954	20.4	4.7	14.2	41	42	0.83	0.62
R6-8PPG-1K	PPG1000,8	95.2	745	165	910	18.1	5.1	16.2	41	44	0.85	0.64
R7-20PPG-1K	PPG1000,20	82.9	460	155	615	25.3	4.7	16.6	29	45	0.92	0.66
R8-50PPG-1K	PPG1000,50	86.4	545	233	778	29.9	9.3	26.6	44	61	0.86	0.82
R9-100PPG-1K	PPG1000,100	65.8	60	97	158	61.8	6.4	74.8	9	63	1.16	0.83
R10-5PPG-4K	PPG4000,5	94.9	790	215	1005	21.4	5.6	15.0	41	42	1.27	0.59
R11-6PPG-4K	PPG4000,6	74.1	715	161	876	18.3	6.3	8.9	44	48	0.91	0.69
R12-7PPG-4K	PPG4000,7	91.6	715	167	882	18.9	6.6	9.5	44	49	0.95	0.72
R13-8PPG-4K	PPG4000,8	96.8	730	174	904	19.3	6.9	9.1	44	47	0.93	0.69
R14−20PPG-4K	PPG4000,20	78.6	530	137	667	20.5	7.7	29.8	33	54	1.53	0.61
R15-50PPG-4K	PPG4000,50	77.6	15	71	86	82.6	9.7	30.5	2	58	1.31	0.94
R16-100PPG-4K	PPG4000,100	56.8	75	76	151	50.4	4.4	80.0	9	59	1.14	1.22
R17-5PDMS	PDMS,5	92.2	700	167	867	19.3	5.0	14.0	38	39	1.83	0.61
R18-6PDMS	PDMS,6	89.2	730	156	886	17.6	6.3	10.1	44	49	0.95	0.71
R19-7PDMS	PDMS,7	88.1	700	214	914	23.4	5.9	8.5	41	50	0.92	0.68
R20-8PDMS	PDMS,8	90.4	700	167	867	19.3	6.6	7.6	41	43	0.92	0.69
R21-20PDMS	PDMS,20	72.9	575	95	670	14.1	4.2	44.8	16	39	2.13	0.79
R22-50PDMS	PDMS,50	64.9	<5	88	93	94.6	58.4	70.8	>1	60	1.37	0.93
R23-100PDMS	PDMS,100	48.3	15	69	84	82.2	11.5	147.8	>1	69	1.91	1.21

[a] Balance is toluene, DVB/porogen = 1/1 v/v. [b] Assuming density poly(DVB) = 1 g cm^{-3}.

contribution.[22] Since PEGs are water-soluble, it was not possible for us to use these in suspension polymerizations, but poly(propylene glycol)s, PPGs, and a poly(dimethylsiloxane), PDMS, have proved to be very useful.

Experimental Section

Materials. Divinylbenzene (DVB) (80% grade), poly(vinyl alcohol) (88% hydrolyzed, $M_n \sim 125\,000$), poly(propylene glycol) 1000 (PPG1000) ($M_n \sim 1000$), and poly(propylene glycol) 4000 (PPG4000) ($M_n \sim 4000$) were from the Aldrich Chemical Co. Toluene was supplied by Bamford Laboratories, azobis(isobutyronitrile) (AIBN) by Acros Organics, poly(dimethylsiloxane) (PDMS) (viscosity 200/100 cSt) by Hopkins and Williams, and sodium chloride by the BDH Co. All materials were used as supplied.

Suspension Polymerizations. These were prepared essentially as reported before using a parallel-sided glass reactor.[9,23] The composition of the aqueous phase was water (1000 mL), poly(vinyl alcohol) (7.5 g), and sodium chloride (33 g). 700 mL of this solution was charged into the reactor. The organic phase was DVB (80% grade) (17.5 mL), porogen (17.5 mL), and AIBN (0.175 g, 1 mol %). The aqueous continuous phase/organic phase ratio was therefore 20/1 v/v, and the monomer/porogen ratio was 1/1 v/v. When an oligomeric coporogen was used, the total volume of porogens was kept fixed at 17.5 mL, and the compositions in Table 1 refer to volume percent of each porogen. Polymerizations were run at 80 °C for 6 h. The resin beads were collected by filtration, washed with water and methanol, and then extracted overnight in a Soxhlet using either acetone (for PPG porogens) or toluene (for PDMS porogen). Finally, the beads were washed with methanol and diethyl ether before drying in a vacuum oven. The resins synthesized are indicated in Table 1.

Instrumentation and Resin Characterization. The chemical composition of resins was confirmed by FTIR spectroscopy and by elemental microanalysis for C% and H%. The latter analyses were performed on a Perkin-Elmer 2400 analyzer and the former on a Perkin-Elmer 1600 series FTIR instrument using a diamond compression cell. The accumulated elemental microanalytical data are shown in Table 1.

The porous morphology of each resin was quantified by N_2 sorption porosimetry using a Micromeritics ASAP 2000 gas adsorption instrument, and the data were manipulated using the software supplied with the instrument. Hg intrusion porosimetry data were also acquired using a Micromeritics Autopore II 9220 and again the dedicated software used to generate appropriate porosity parameters.

Solvent uptake data for each resin using both toluene and *n*-hexane (as typical swelling and nonswelling solvents, respectively, for styrene-based resins) were determined gravimetrically and expressed as g of solvent per g of dry resin, using a sinter stick and centrifugation (3 min at 3000 rpm) to remove excess solvent.[24] Resins were contacted with each solvent for 3 h to allow equilibrium to be attained prior to centrifugation. A summary of the data obtained appears in Table 1.

Scanning electron microscopic (SEM) analysis of resins was carried out on a JEOL 6400 scanning electron microscope operating at 10 kV. Samples were gold-coated.

Results and Discussion

Resin Syntheses. Suspension polymerizations were completed without experimental problems for all three oligomeric porogens (PPG1000, PPG4000, and PDMS) across the full range of composition (0−100 vol %) explored. In each case spherical beaded products were obtained without e.g. any complications of high viscosity even when the oligomers were employed at high volume fraction of the porogen (50 and 100%). Typical bead diameters were in the range 200−500 μm and were little affected by the porogen employed.

The yields of high-quality beads were also very good (Table 1) but did fall when each oligomeric porogen was employed at 50 and 100 vol %. The main reason for this was the presence of a "fines" component dispersed in the beads, necessitating repetitive washing, with concomitant loss of product. Indeed, even after prolonged cleaning in an ultrasonic bath some of this component could not be removed entirely and seemed to be intimately associated with the beads (see SEM later). With use of 100 vol % of oligomer the isolated yields fall in the series PPG (1000), 65.8%; PPG(4000), 56.8%; PDMS, 48.3%, and so the chemical structure and molar mass

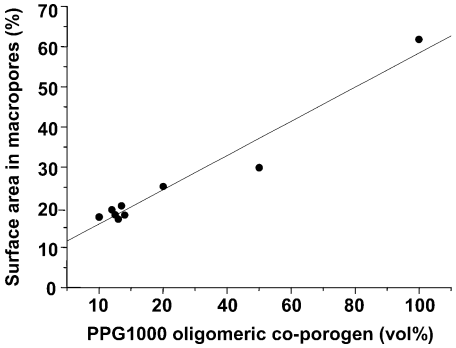

Figure 2. Plot of surface area of macropores (%) vs PPG1000 coporogen content (vol %) in dry state poly(DVB) resins.

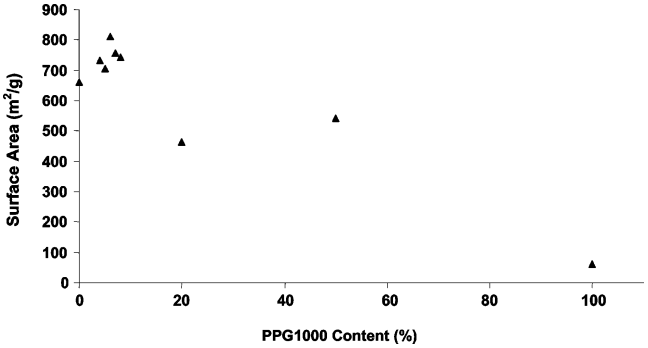

Figure 3. Plot of surface area (N_2 BET) vs PPG1000 coporogen content (vol %) of dry state poly(DVB) resins showing maximum ~6 vol % PPG1000.

are both factors associated with the production of "fines" and the fall in yield of high-quality beads.

The elemental microanalyses of all our products consistently afforded contents of carbon and hydrogen in a range 89.8−91.5% and 7.4−8.2%, respectively, which agree well with the theoretical values calculated by poly(DVB) (C, 92.3%; H, 7.7%). These data suggest that little if any of the oligomeric porogens are retained within the resins. Indeed, the FTIR spectra of all products displayed no evidence of the bands characteristic of the oligomers.

Resin Porosity Characteristics. a. Surface Area. The surface area data for all resins calculated from the N_2 sorption isotherms using the Brunauer, Emmet, and Teller[25] (BET) treatment and from the Hg intrusion data are shown in Table 1.

In the case of the N_2 sorption experiments the surface area was calculated from the adsorption branch of the isotherm (see pore size later). In comparing and contrasting these data sets, it is important to bear in mind that the N_2 sorption experiment does not probe effectively pores say >200 nm while the Hg intrusion experiment likewise may not account accurately for pores say <20 nm. The results in Table 1 therefore show both sets of surface area data, and making the assumption that these are additive, the total surface areas are also displayed along with the surface area (%) associated with macropores (from the Hg intrusion data).

Although there is some scatter in the data, the fraction of surface area associated with large pores clearly rises as the level of oligomeric porogen employed is increased, and indeed for PPG1000 there seems to be a linear relationship (Figure 2). Indeed, even if the N_2 sorption and Hg intrusion derived surface area data are not strictly additive, this trend is still valid.

Another important trend is that as the level of oligomeric porogen used is increased, the N_2 sorption data derived (BET) surface area fall (Figure 3). This is as expected since the presence of the oligomer would be expected to induce phase separation earlier than would be the case with pure toluene as the porogen, which in turn would favor the production of larger pores, lowering the overall surface area.

Indeed, the pairs of data computed from the N_2 adsorption isotherms and the Hg intrusion experiments for resins prepared with 100 vol % oligomeric porogens (R9, R16 and R23) become very similar. Particularly interestingly, however, in the case of all three oligomeric porogens, the effect of adding low levels of these is to initially *increase* the surface area (BET) (e.g., Figure 3 for PPG1000 coporogen). The maximum values are achieved with 5−6 vol % of oligomer, and the increase

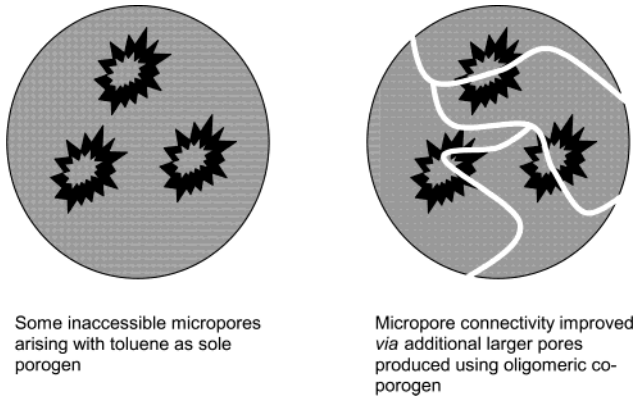

Figure 4. Schematic representation of improved micropore connectivity in poly(DVB) resins arising when low levels of an oligomer coporogen are employed with toluene as solvent porogen.

in surface area observed is very significant in each case ~150 $m^2\ g^{-1}$ with PPG1000, ~130 $m^2\ g^{-1}$ with PPG4000, and ~70 $m^2\ g^{-1}$ with PDMS. Since added oligomer is unlikely to increase the proportion of small pores, the most plausible explanation for this effect is that the oligomer causes changes in the morphology that allows previously inaccessible, or closed, small pores to be made available; i.e., the connectivity of the previously existing small pores is improved, presumably via the creation of an embryonic network of much larger pores. Indeed, this argument is confirmed by examination of the N_2 sorption derived cumulative surface area/pore size data for resins R1-TOL prepared using toluene only as the porogen and R4-6PPG-1K prepared with 6 vol % PPG1000 coporogen. The latter shows an increase of ~20% in the contribution to the surface area from small pores along with the emergence of a definite mesopore fraction. This is shown schematically in Figure 4. We believe that this observation may have significant technological significance e.g. in improving the performance of high surface area resin sorbents.

b. Average Pore Size. Because of the experimental limitations on both the N_2 sorption derived parameters and those from Hg intrusion experiments, it is important to consider both data sets. The average Barret, Joyner, and Halenda[26] (BJM) pore sizes derived from the N_2 adsorption isotherms and the corresponding average pore sizes from Hg intrusion measurements are shown in Table 1. As expected, the latter are systematically larger than the former because the Hg intrusion data omits the smallest pores, and the N_2 adsorption data omit the largest pores. Overall, however, though

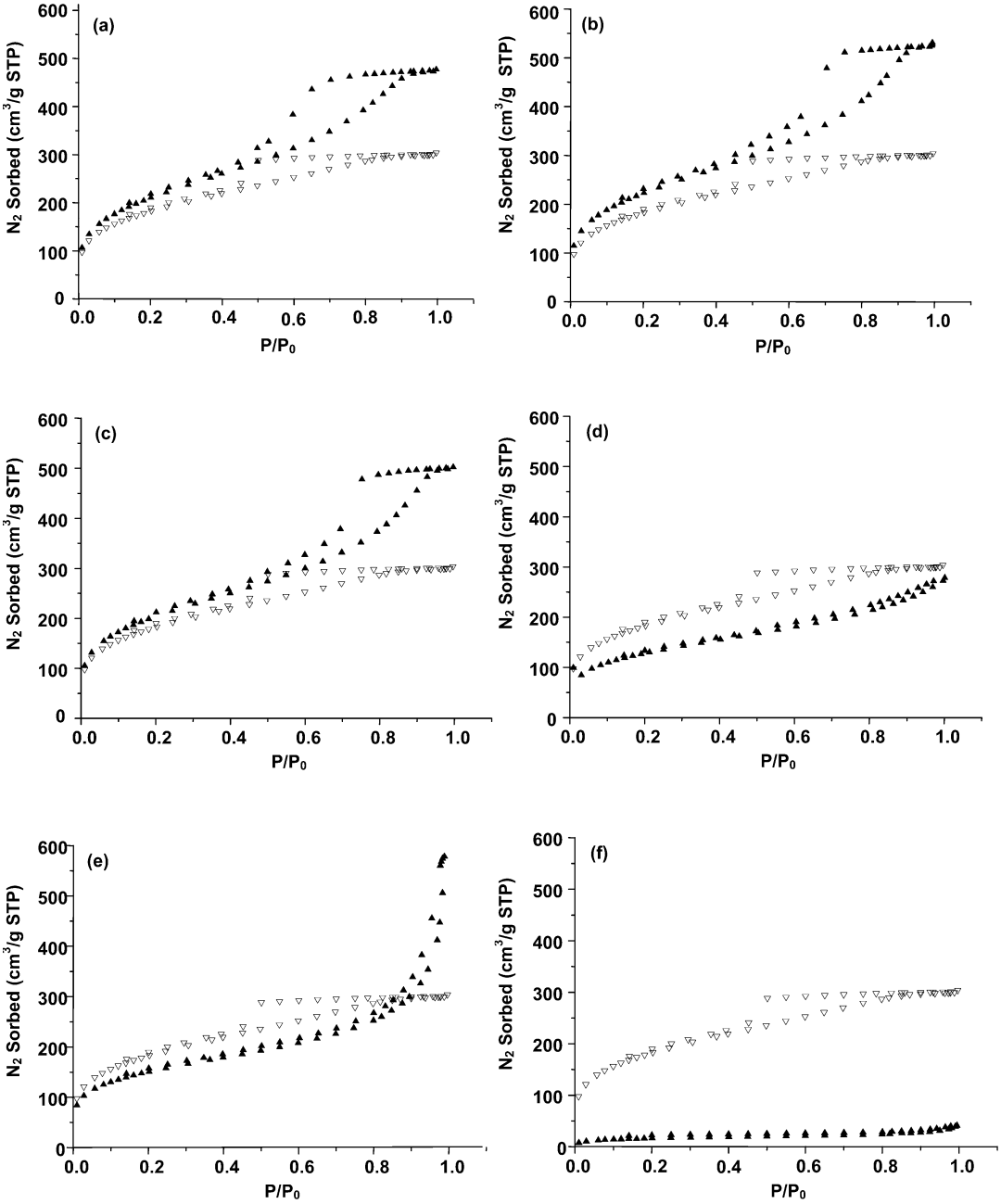

Figure 5. N_2 adsorption/desorption isotherms for poly(DVB) resins: ▽, PPG1000 coporogen (a) 4, (b) 6, (c) 8, (d) 20, (e) 50, and (f) 100 vol %; ▲, toluene porogen 100 vol %.

there is a little scatter, average pore sizes increase as the level of oligomeric porogen employed is increased.

The resin sets R10−R16 and R17−R23 prepared using varying levels PPG 4000 and PDMS, respectively, as coporogens show similar trends to those described above for PPG 1000 as coporogen.

Hysteresis Behavior in N_2 Adsorption/Desorption Isotherms. Since low levels of oligomeric coporogen tend to increase the accessible surface area (N_2 BET) in each set of resins, it was thought that this improved connectivity might be manifest in a reduced hysteresis effect in the N_2 adsorption/desorption isotherms. The latter are shown in Figure 5 for the series of resins R2−R9 prepared using PPG 1000. The data for R1 prepared with toluene porogen alone are shown in each Figure 5, and indeed the desorption arm of the isotherm shows a sharp fall at $P/P_0 \sim 0.5$, indicative of some restricted pore connectivity and sudden desorption of N_2 from "ink well" and other restricted pores. The corresponding isotherm for resin R2 (Figure 5a) prepared with 4 vol % PPG 1000 in toluene shows a higher N_2 sorption in the plateau region ($P/P_0 \sim 0.2-0.5$), which translates into a higher surface area (N_2 BET), and is consistent with the argument that previously inaccessible small pores (in R1) have become available as a result of the oligomeric coporogen, providing an embryonic network of larger pores (Figure 4).

However, the isotherm for R2 also shows an enlarged hysteresis loop above $P/P_0 \sim 0.5$, suggesting that the larger pores created are themselves subject to connectivity limitations. Clearly, therefore, these hysteresis effects have to be considered carefully, and no one simple explanation can accommodate all the experimental data. With resin R4 where the PPG 1000 content was increased to 6 vol %, the N_2 sorption isotherm (Figure 5b) is shifted well above that for resin R1 at all

values of P/P_0, and this is reflected in the maximum value of surface area (N2 BET) of 815 $m^2\ g^{-1}$ calculated for this resin. Again, however, though the accessibility of the small pores seems to be increased, a significant hysteresis loop remains in the isotherm, showing that connectivity limitations are by no means all eliminated. The data for resin R6 prepared with 8 vol % PPG 1000 are shown in Figure 5c, and the isotherm has now moved down to partially overlap with that of resin R1. This trend continues with the data for resins R7−R9 as the PPG 1000 content is increased to 20, 50, and 100 vol %, respectively. The sorption isotherms fall progressively further and further below that of resin R1 (Figure 5d−f), with the corresponding surface areas (N_2 BET) likewise declining steeply as the small pores disappear and are replaced by large pores in these latter resins. The isotherms also show a continuous rise as $P/P_0 \rightarrow 1$, most obvious with resin R8 (Figure 5d) indicative of the presence of a significant population of macropores. Interestingly as well the hysteresis effect in the adsorption/desorption cycle disappears, suggesting a good interconnection of the pore structure that is formed.

Pore Size Distributions. A much better representation of the pore structure in resins is of course given by the pore size distribution. The latter was computed for each resin using the BJH treatment[26] of the N_2 adsorption isotherm and from the Hg intrusion data assuming the pores to be cylindrical.[27,28] To give a comprehensive picture, it is necessary to overlap these two data sets. The results for the set of resins R17−R23 prepared using PDMS as the oligomeric coporogen are shown in Figure 6. In the case of the N_2 sorption experiments the data from the adsorption branch of the isotherm were used in this calculation since it is now generally accepted that the desorption data are compromised by artifacts arising from imperfect pore connectivity. The pore size distribution curves for resin R1 prepared with toluene only as the porogen are shown in Figure 6a.

The N_2 sorption derived data show a large population of pores in the micropore region extending to the lower part of the mesopore region. The Hg intrusion derived data suggest a large mesopore population but fails to detect the micropore fraction at all. Most importantly, however, the latter plot shows a complete absence of macropores. Overall, this picture is much as expected when using toluene as the sole porogen with 100% DVB. In the case of resin R18 prepared with 6 vol % PDMS as coporogen the main change in the data (Figure 6b) is a more significant mesopore population displayed in the N_2 sorption derived data. Indeed, the agreement between the N_2 adsorption and Hg intrusion derived data in the mesopore region is remarkable. This increase in the mesopore range may itself account for the increase in the surface area (N_2 BET) in resin R18 relative to R1, but more likely is also responsible for increasing access to previous inaccessible micropores. The pore size distribution curves for resin R20 (Figure 6c) suggest further growth in the mesopore region toward its upper limit, but the agreement between the two data sets is less good here. A major change is apparent, however, in the data for resin R21 prepared with 20 vol % PDMS (Figure 6d). Both sets of data show a very significant loss of pores in the mesopore region, with the N_2 sorption derived data showing a retention of a significant micropore population, and the Hg intrusion derived data showing the arrival of a significant macropore fraction. This resin does indeed have a bimodal distribution of pore sizes as originally targeted in our design rationale (Figure 1C). The resin also retains a very significant surface area ∼530 $m^2\ g^{-1}$ (N_2 BET). The distribution curves for resins R22 and R23 (Figure 6e,f) are similar and show essentially no contribution from pores in the micropore region, a very low mesopore fraction, along with a dominant macropore population. The surface area is very low in each case 5−15 $m^2\ g^{-1}$ (N_2 BET). The peak in the macropore distribution shifts from ∼300 to ∼600 nm in moving from 50 to 100 vol % PDMS coporogen with the breadth of the distribution being rather narrow in the latter case. Hence essentially in this resin, R23, our second design rationale (Figure 1A) has also been realized.

Similar changes in the pore size distributions have been observed in the other sets of resins R2−R9 and R10−R16 prepared with the two PPG oligomeric coporogens.

Pore Volumes. For some applications of porous resins a particularly important parameter is the pore volume. N_2 sorption data allow the BJH pore volume (and thence percent porosity) to be calculated, Hg intrusion allows a percent porosity to be deduced, and solvent uptake measurements allow the volume or mass of solvent imbibed to be measured. These data are summarized for all the resins in Table 1. It is important to appreciate that each of these experiments have their limitation, and each in effect provides a different measure of pore volume or porosity. All resins were prepared with an equal volume of porogen(s) relative to DVB, and as a very approximate guide, removal of the porogen from the product resin should remove ∼50% of the volume of each bead. Assuming the polymer phase and the porogen have the same density (say ∼ unity) 1 g of dry beads should have ∼1 cm^3 of pores; i.e., the porosity should be ∼50% with the bead having an apparent density of 0.5 g cm^{-3}.

Considering first the BJH pore volume data, superficially resins R9, R15, R16, R22, and R23 appear to have very low values because the pore volume resides primarily in macropores and the N_2 sorption technique does not probe these effectively. Microporous resin R1 yields a value of 0.4 $cm^3\ g^{-1}$, significantly below the order of magnitude value of 1 $cm^3\ g^{-1}$ argued above. Hence, it seems that significant contraction takes place when this resin is finally isolated and dried. This is confirmed by the percent porosity datum from the Hg intrusion experiment where the figure is ∼33%, again below the order of magnitude estimate of 50%. Perhaps more surprising, even when this resin is rewetted with either toluene or *n*-hexane, the solvent uptake data 0.45 g/g (toluene) and 0.34 g/g (*n*-hexane) remain significantly lower than what might have been expected. This tends to confirm that some permanent contraction occurs during synthesis, isolation, and drying of this resin. In contrast, the remaining resins prepared with the oligomeric coporogens show significantly larger BJH pore volumes, typically ∼0.7−0.8 $cm^3\ g^{-1}$ and higher porosities (Hg intrusion data). With the latter data there is also a systematic increase in percent porosity with increase in vol % of oligomeric coporogen used, and this suggests that this component of the porogen mixture endows the resin with greater resistance to shrinkage on isolation and drying.

A comparison of the toluene and *n*-hexane uptake is valuable because the latter solvent would be expected to fill pores whereas the former would be expected to

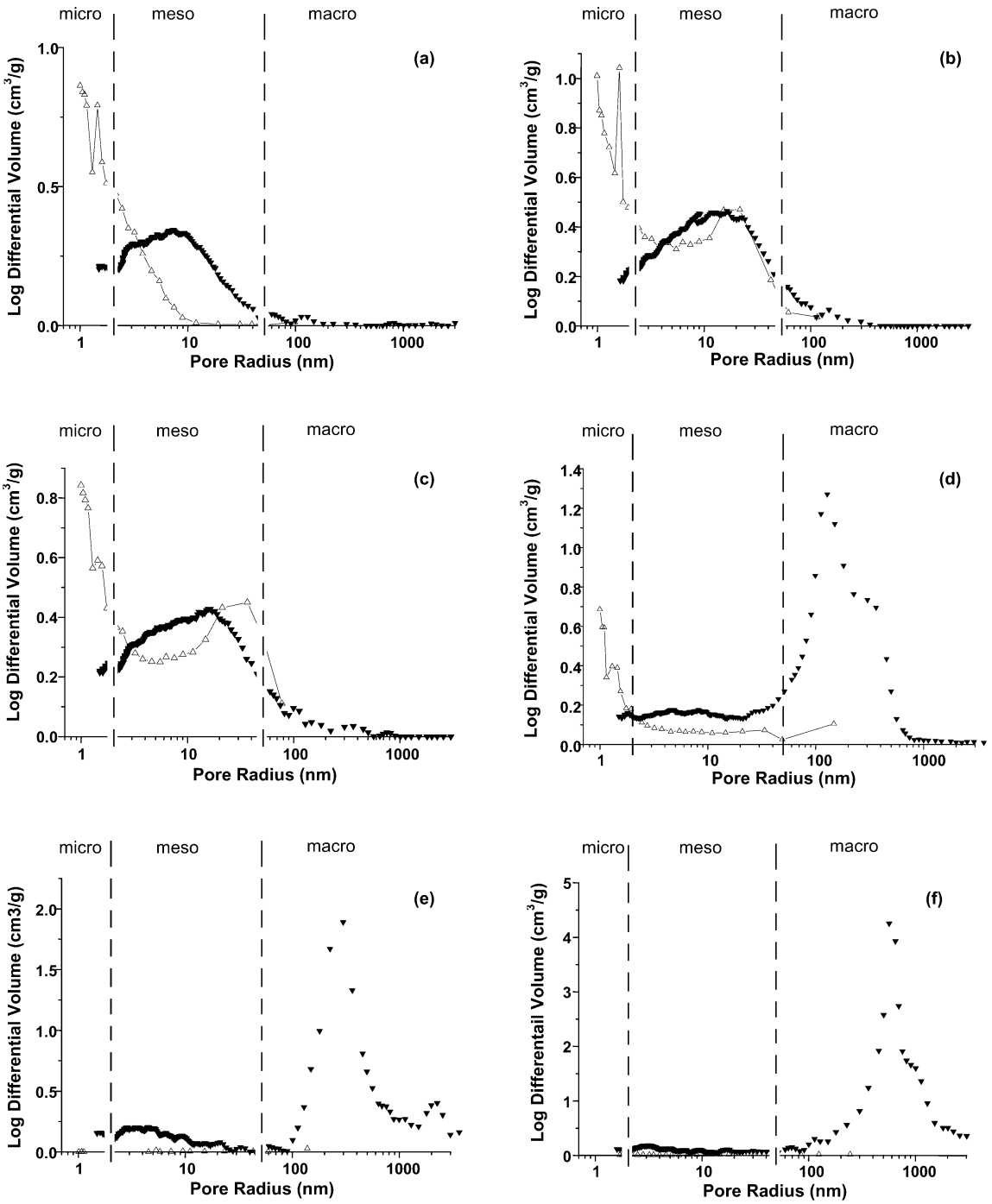

Figure 6. Combined N_2 adsorption-derived (▼) and Hg intrusion-derived (△) pore size distribution for poly(DVB) resins: (a) toluene porogen 100 vol %; (b) PDMS coporogen 6 vol %; (c) PDMS coporogen 8 vol %; (d) PDMS coporogen 20 vol %; (e) PDMS coporogen 50 vol %; (f) PDMS porogen 100 vol %.

fill pores but also solvate the polymer matrix and potentially swell this. Any solvent swelling may well increase the pore volume. In any event the consistently higher toluene uptake data relative to that of *n*-hexane suggests that resin swelling does occur to varying degrees. At the highest levels of vol % oligomeric coporogen the *n*-hexane uptake typically approaches 1 g/g, which reflects the level of porogen(s) used in the resin preparations. In the case of toluene the uptake data typically rise above this figure, again suggesting that swelling, as well as pore filling, arises with this solvent.

Overall all the resins prepared with oligomeric coporogen retain very substantial pore volumes.

Scanning Electron Microscopy (SEM). Scanning electron micrographs of some representative resins (R1, R18, R21, and R23) are shown in Figure 7.

This series were prepared with 0, 6, 20, and 100 vol % PDMS as oligomeric coporogen and represent the full range of morphology changes detected in the N_2 sorption and Hg intrusion characterization data. Resin R1 (Figure 7a) shows a very fine surface texture, which is rather uniform, and indeed the resolution of the SEM is too poor to reveal the microporous structure. Resin R18 (Figure 7b) shows a marginally rougher texture somewhat less uniform, but again definitive pore structure is not apparent. Resin R21 (Figure 7c), however, reveals a clear macropore population even at the bead

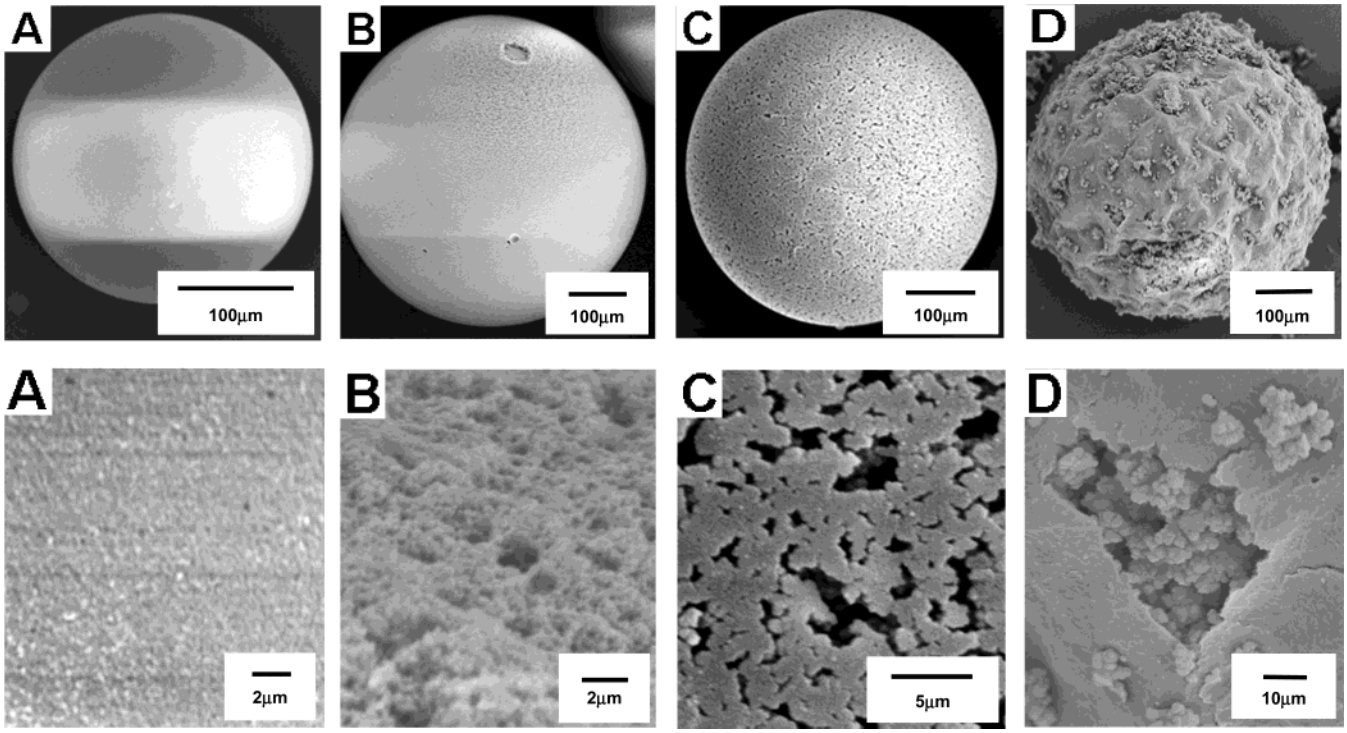

Figure 7. Scanning electron micrographs of poly(DVB) resins prepared using (A) toluene porogen 100 vol %, (B) PDMS coporogen 6 vol %, (C) PDMS coporogen 20 vol %, and (D) PDMS porogen 100 vol %.

surface, and the corresponding micropore fraction, shown earlier to be present in this bimodally porous resin (Figure 6d), is presumably associated with the polymer microgel particles which can be seen. Superficially therefore this resin resembles very closely the cartoon (Figure 1C) in our original design concept. Resin 23 (Figure 7d) shows a rough contaminated surface with fragments associated with it. The recovered yields of resins R9, R16, and R23, each prepared with 100 vol % oligomeric porogen, were all adversely affected by the presence of fines, and these are seen clearly adhering to the surface of this resin. The contamination is however superficial as the high-magnification SEM image of this resin shows access to a discrete macroporous structure. Some similarity (below the surface) of this resin, R23 (Figure 7d), with resin R21 (Figure 7c) is apparent, but the major difference is that the polymer microgel phase in R23 is essentially nonporous, such that overall R23 has a unimodal macroporous morphology. Overall, therefore these SEM images agree extremely well with the N_2 sorption and Hg intrusion derived porosity data.

Conclusions

The original aim of this work was to evaluate the use of oligomeric species as porogens, and coporogens with toluene, in the synthesis of poly(DVB) resins. In our idealized design rationale (Figure 1A) early phase separation of the oligomer used as sole porogen was expected to yield a resin with macropores only, and this has proved to be the case in practice. Indeed, surprisingly narrow pore size distributions in the near micron range have been achieved. The oligomeric nature of these species also means that high levels can be used (generating good pore volumes) without giving rise to highly viscous polymerization mixtures which is the case with high molecular weight polymer porogens (used alone). The other idealized design rationale (Figure 1C) we had was to use oligomers as coporogens with toluene and hence induce phase separation in two stages: an early event in which the oligomer phase separates to produce (eventually) macropores and a late event in which the toluene phase separates to produce micropores. Optimally a bimodal pore size distribution might be achieved. This hypothesis was, and indeed remains, an oversimplistic one in that being able to select all components such that they behave separately as we desired is an almost impossible undertaking. In the event low levels of oligomeric coporogen have been found to offer a bonus in terms of increasing the surface area of resins prepared with a porogen/cross-linker composition already known to yield high surface areas. This increase in surface area is significant and arises from the increase in the population of mesopores in these resins. The latter probably make previously inaccessible or closed micropores accessible, while also contributing directly to the surface area themselves. It is doubtful however that in this composition range of porogen/coporogen that the latter act independently of each other since the components used, toluene and the PPG and PDMS coporogens, are readily miscible. Despite this, when the oligomeric coporogen is used at 20 vol %, then the morphology of the resulting resin does display a discrete bimodal pore size distribution with little contribution in the mesopore range. It is tempting to suggest therefore that the idealized design rationale (Figure 1C) we had in this case was also achieved in practice.

References and Notes

(1) Farben Fabraken Bayer, German Patent DEI 045102, 1957.
(2) The Rohm and Haas Co., British Patents GB 932125 and 932126, 1959.
(3) The Permutit Co., British Patents GB 849112 and 860695, 1960.
(4) *4.Ion Exchangers;* Dorfner, K., Ed.; de Gruyter Pubs: Berlin, Germany, 1991.

(5) Ley, S. V.; Baxendale, J. R.; Bream, R. N.; Jackson, P. S.; Leach, A. G.; Taylor, S. J. *J. Chem. Soc., Perkin Trans. 1* **2000**, 3815−4195.
(6) *6.Polymeric Materials in Organic Synthesis and Catalysis*; Buchmeiser, M. R., Ed.; Wiley-VCH: Darmstadt, 2003.
(7) *7.A Practical Guide to Combinatorial Chemistry;* Czarnik, A. W., DeWitt, S. H., Eds.; American Chemical Society: Washington, DC, 1997.
(8) Albright, R. L. *React. Polym.* **1986**, *4*, 155−174.
(9) Sherrington, D. C. *Chem. Commun.* **1998**, 2275−2286.
(10) Okay, O. *Prog. Polym. Sci.* **2000**, *25*, 711−779.
(11) Seidl, J.; Malinsky, J.; Dusek, K.; Heitz, W. *Adv. Polym. Sci.* **1967**, *5*, 113−213.
(12) Sederel, W. L.; De Jong, G. J. *J. Appl. Polym. Sci.* **1973**, *17*, 2835−2846.
(13) Poineseu, Ig. C.; Vlad, C.-D. *Eur. Polym. J.* **1997**, *33*, 1515−1521.
(14) Horak, D.; Labsky, J.; Pilar, J.; Bleha, M.; Pelzbauer, Z.; Svec, F. *Polymer* **1993**, *34*, 3481−3489.
(15) Ferreira, A.; Bigan, M.; Blondeau, D. *React. Funct. Polym.* **2003**, *56*, 123−136.
(16) Cheng, C. M.; Micale, F. J.; Vanderhoff, J. W.; El-Aasser, M. S. *J. Polym. Sci., Part A: Polym. Chem.* **1992**, *30*, 235−244, 245−256; *J. Colloid Interface Sci.* **1992**, *50*, 549−558.
(17) Wang, Q. C.; Svec, F.; Fréchet, J. M. J. *J. Polym. Sci., Part A: Polym. Chem.* **1994**, *32*, 2577−2588.
(18) Lewandowski, K.; Svec, F.; Fréchet, J. M. J. *J. Appl. Polym. Sci.* **1998**, *67*, 597−607.
(19) Ugelstad, J.; Kaggerud, K. H.; Hansen, F. K.; Berger, A. *Makromol. Chem.* **1979**, 737−742.
(20) Palm, A.; Novotny, M. V. *Anal. Chem.* **1997**, *69*, 4499−4507.
(21) *21.Monolithic Materials: Preparation, Properties and Applications;* Svec, F., Tennikova, T. B., Deyl, Z., Eds.; Elsevier: Amsterdam, 2003.
(22) Viklund, C.; Nordström, A.; Irgum, K.; Svec, F.; Fréchet, J. M. J. *Macromolecules* **2001**, *34*, 4361−4369.
(23) van Berkel, P. M.; Sherrington, D. C. *Polymer* **1996**, *37*, 1431−1435.
(24) Pepper, K. W.; Reichenburg, D.; Hale, D. K. J. *J. Chem. Soc.* **1952**, *4*, 3129−3131.
(25) Brunauer, S.; Emmet, P. H.; Teller, E. *J. Am. Chem. Soc.* **1938**, *60*, 309−319.
(26) Barret, E. P.; Joyner, L. G.; Halenda, P. P. *J. Am. Chem. Soc.* **1951** *73*, 373−380.
(27) Washburn, E. W. *Proc. Natl. Acad. Sci. U.S.A.* **1921**, *7*, 115−116.
(28) *28.Analytical Methods in Fine Particle Technology*; Webb, P. A., Orr, C., Eds.; Micromeritics Instrument Corp.: Norcross, GA, 1977.

MA0491053